Finite element formulation for Maxwell's equations with space dependent electric properties

Application to time domain reflectometry probe

André Chambarel* — Evelyne Ferry*

* *Laboratory of Complex Hydrodynamics*
33, rue Louis Pasteur F-84000 AVIGNON
andre.chambarel@univ-avignon.fr

ABSTRACT. *The Time Domain Reflectometry -TDR- probe is a new technique applied to moisture measurement. It is a wave guide constituted by two or three parallel metallic rods stuck in the ground. An electromagnetic wave propagates all along the wave guide and crosses a variable electric properties medium. In that way the reflecting wave is disrupted and we detect the electric singularities. We study the transverse magneti- mode. We simulate this wave guide in this medium thanks to the Finite Element Method and present the used matricial structure. For time integration we compare a semi-implicit or Runge-Kutta method with variable time-step. This process is driven by the Automatic Multigrid System with an unknown time-dependent number..*

RÉSUMÉ. *La sonde de réflectométrie temporelle est une nouvelle technique appliquée à la mesure d'humidité. C'est un guide d'ondes constitué par deux ou trois tiges métalliques parallèles plantées dans la terre. Une onde électromagnétique se propage le long du guide d'ondes dans un milieu à propriétés électriques variables. Dans ces conditions, la réflexion de l'onde est perturbée et détecte les singularités. Nous étudions le mode TM et nous simulons le guide d'ondes par la méthode des Eléments Finis dont nous donnons la formulation matricielle. Pour l'intégration temporelle nous comparons une méthode semi-implicite avec la méthode de Runge-Kutta avec un pas de temps variable. Le calcul est piloté par AMS avec un nombre d'inconnues fonction du temps.*

KEY WORDS : *Finite Element, Maxwell's equations, electromagnetic waves, waves guide.*

MOTS-CLÉS : *éléments finis, équations de Maxwell, ondes électromagnétiques, guides d'ondes.*

Revue européenne des éléments finis. Volume 9 – n° 8/2000, pages 941 à 967

1. Introduction

Water resource management for plants is becoming an increasingly acute problem. This is associated with pollution phenomena usually caused by fertilizers. It is therefore essential to have a precise idea as to the soil's moisture content, both at surface and underground levels. Various techniques have been used to this effect, e.g. the uneasy technique of sampling. Then in the 60's and 70's neutron probes [VAN 63] were used, that - beyond the poor level of accuracy - offered the major drawback of appealing to a radioactive source. A number of current research program are investigating new technologies usually based on electrical measures. Resistive [FLE 85] and capacitive [GAU 93] probes can be offered as examples, that set problems of both reliability and accuracy. The latest generation of instruments [SPA 95] under development is based on Time Domain Reflectometry -TDR-. These instruments come as two or three parallel metal rods driven into the ground down to little over three feet - or 1 m -. An electrical impulse is applied to the end bit above ground surface. The impulse propagates along the rods. Measurement and processing of the signal obtained by reflection should theorically allow the determination of local moisture levels. The 1D model used up to now in the study of our device is that of the electric line represented in Figure 1 [TOD 98].

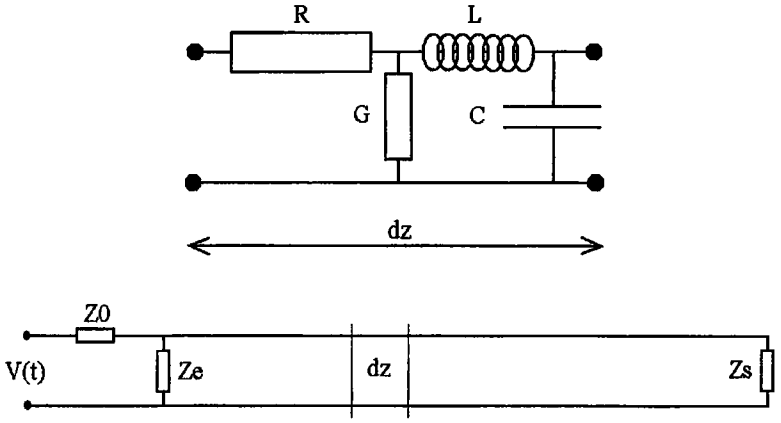

Figure 1. *The electric line scheme*

$$\frac{\partial I}{\partial z} = -C.\frac{\partial V}{\partial t} - G.V$$

$$\frac{\partial V}{\partial z} = -L.\frac{\partial I}{\partial t} - R.I$$

The line's 1D mathematical model is governed by a partial differential system called "telegraphists equations". These equations are dealt with in a traditional way through time or frequency approach. In the case of Time Domain Reflectometry though, there is no specific problem. The difficulty in fact lies in the perfect knowledge of the values of parameters (R,L,C,G,Zs), in particular in their relationship with soil moisture profile [DOS 97]. The impedances Z0 and Ze are given by the electric source properties. Besides, this simplified 1D model neither, for example, takes into account the various propagation modes of electromagnetic waves, nor the cut frequency, nor again the local ratings of soil moisture. So to improve the model, an approach based on the Maxwell's equations appears necessary, so that we may have at hand a numerical tool that will provide the "telegraphists equations" with reliable data. In this way, we built a 2D model for the TDR probe.

2. General presentation of the model

2.1. *Geometrical model of the 2D TDR probe*

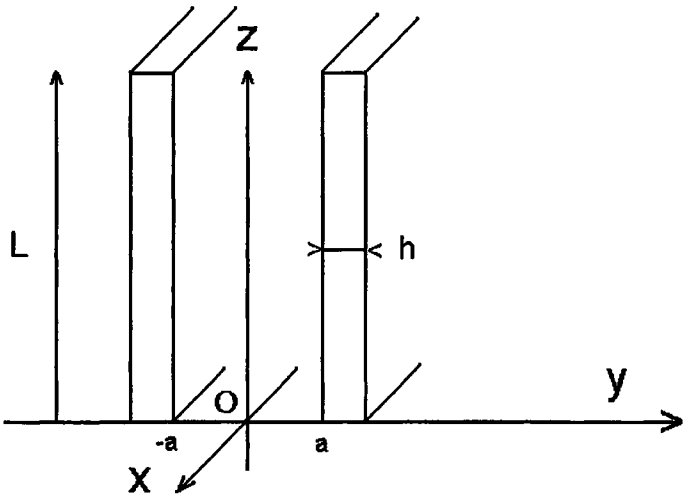

Figure 2. *Geometrical model*

The electric line (Figure 2) is represented by two parallel plate electrodes and the electric conductivity of these is infinite. The free space around the electrodes can be an ohmic conductor. In the Transverse Magnetic mode -TM-, the electromagnetic field is :

$$\vec{H} = \begin{Bmatrix} H_x \\ 0 \\ 0 \end{Bmatrix} \quad \text{and} \quad \vec{E} = \begin{Bmatrix} 0 \\ E_y \\ E_z \end{Bmatrix}$$

2.2. *Maxwell's equations*

With the usual notations the Maxwell's equations are formulated as follows [FLE 91] :

$$\overrightarrow{\text{curl}}\,\vec{E} = -\frac{\partial \vec{B}}{\partial t} \qquad \text{div}\,\vec{B} = 0 \qquad [1]$$

$$\overrightarrow{\text{curl}}\,\vec{H} = \vec{J} + \frac{\partial \vec{D}}{\partial t} \qquad \text{div}\,\vec{D} = \rho \qquad [2]$$

If we are inside a material, we have the following laws:

$$\begin{aligned} &\vec{J} = [\gamma]\vec{E} = \gamma_0 \cdot [\gamma_r]\vec{E} \qquad \text{(Ohm's law)} \\ &\vec{D} = [\varepsilon]\vec{E} = \varepsilon_0 \cdot [\varepsilon_r]\vec{E} \\ &\vec{B} = [\mu]\vec{H} = \mu_0 \cdot [\mu_r]\vec{H} \end{aligned} \qquad [3]$$

Notation [.] can be a space dependent tensor.

For a numerical model we prefer to use adimensional equations. In this way we define reference quantities :

l reference length

$c = \dfrac{1}{\sqrt{\varepsilon_0 \cdot \mu_0}}$ reference velocity

$H_0 = E_0 \cdot \sqrt{\dfrac{\varepsilon_0}{\mu_0}}$ reference magnetic field

The characteristic time is $\tau = \dfrac{l}{c}$

The variables of the Maxwell's equations become:

$$x_i = \frac{x_i'}{l} \qquad t = \frac{t'}{\tau}$$

$$H_i = \frac{H_i'}{H_0} \qquad E_i = \frac{E_i'}{E_0}$$

The Maxwell's equations show a non dimensional parameter:

$$Rm = \gamma_0 . \mu_0 . l . c$$

called the *magnetic Reynolds' number.*

The non dimensional Maxwell's equations become:

$$[\mu_r] \frac{\partial \vec{H}}{\partial t} = -\overrightarrow{\text{curl}\, E} \qquad \text{div}([\mu_r]\vec{H}) = 0 \qquad [4]$$

$$[\varepsilon_r] \frac{\partial \vec{E}}{\partial t} = -\overrightarrow{curl\ H} - Rm\ .[\gamma_r]\vec{E} \qquad div\ ([\varepsilon_r]\vec{D}) = 0 \qquad [5]$$

By using the canonical scalar product equations [4] and [5] are as follows [FLE 91] :

$$\frac{\partial}{\partial t}\left(\frac{\vec{B}.\vec{H}}{2} + \frac{\vec{D}.\vec{E}}{2}\right) = -\vec{H}.\overrightarrow{\text{curl}E} + \vec{E}.\overrightarrow{\text{curl}H} - Rm.\left([\gamma_r]\vec{E}.\vec{E}\right) \qquad [6]$$

$$\frac{\partial}{\partial t}\left(\frac{\vec{B}.\vec{H}}{2} + \frac{\vec{D}.\vec{E}}{2}\right) = -\text{div}\left(\vec{E}\times\vec{H}\right) - Rm.\left([\gamma_r]\vec{E}.\vec{E}\right) \qquad [7]$$

where

$$w = \left(\frac{\vec{B}.\vec{H}}{2} + \frac{\vec{D}.\vec{E}}{2}\right) \qquad \text{and} \qquad \vec{S} = \vec{E}\times\vec{H} \qquad [8]$$

are respectively the adimensional volumic energy and the Poynting vector.

2.3. *Boundary conditions*

The boundary conditions at the electric conductor - i.e. electrodes - can be written :

$$\vec{E} \times \vec{n} = \vec{0}$$

or

$$\left\{ \begin{array}{l} \left(\vec{E}\right)_{\text{tangential}} = 0 \\ \left(\vec{E}\right)_{\text{normal}} = \dfrac{\sigma}{\varepsilon} \text{ (free value)} \end{array} \right\}$$

In that way we can also calculate surfacic charge density σ.

At initial time, we apply a constant electric potential difference between the electrodes. The electric loading can be written :

$$\vec{E} = \left\{ \begin{array}{c} 0 \\ E_0(x, y, z = 0, t) \\ 0 \end{array} \right\}$$

where E_0 is in this case a constant value.

For the other boundary conditions a long way away from the electric line, we must choose :

$$\vec{E} \times \vec{n} = \vec{0}$$

In all cases of TDR procedure, the electromagnetic wave never reaches that boundary because we only study the first reflection in the wave guide for electric properties detection.

The magnetic field value is free because the Maxwell's equations are an hyperbolic system. At the electrodes, we can calculate line current I by the Ampere's theorem with the superficial current density J_S :

$$\vec{H} \times \vec{n} = \vec{J}_S \qquad \text{and} \qquad I = \int_0^1 \left(\vec{J}_S\right)_z .dx = \int_0^1 H_X .dx$$

The initial condition is zero.

3. Finite Element formulation

The Galerkin's Finite Element method is applied to Maxwell's equations in an isotropic medium. In our formulation, the electric properties of the medium can be written:

$$[\mu_r]=\mu_r.[I] \qquad [\varepsilon_r]=\varepsilon_r.[I] \qquad [\gamma_r]=\gamma_r.[I]$$

3.1. *Weak formulation* [ASS 93]

Let (Ω) an open regular space of R^{n_dim} with a regular boundary (Γ) C^0 or C^1 for example. If T is a positive real number we define :

$$\Omega_T = \Omega \times]0,T[$$
$$\Gamma_T = \Gamma \times]0,T[$$

We define also the Hilbert's space (V) :

$$(V)=\left(H^1_{(\Omega)}\right)^{2.n\_dim}$$

where $H^1(\Omega)$ is the following Sobolev's space:

$$H^1_{(\Omega)}=\left\{u \in L^2_{(\Omega)}, \frac{\partial u}{\partial x_i} \in L^2_{(\Omega)}\right\}$$

Let the vectors of space (V):

$$\left(\overrightarrow{W_H}, \overrightarrow{W_E}\right) \quad \text{and} \quad \left(\vec{E}, \vec{H}\right)$$

With the previous scalar product, the weighted residual method can be written:

$$\int_{(\Omega)} \overrightarrow{W_H}.\mu_r.\frac{\partial \vec{H}}{\partial t}.d\Omega = -\int_{(\Omega)} \overrightarrow{W_H}.\overrightarrow{curl}\,\vec{E}.d\Omega \qquad [9]$$

$$\int_{(\Omega)} \overrightarrow{W_E}.\varepsilon_r.\frac{\partial \vec{E}}{\partial t}.d\Omega = \int_{(\Omega)} \overrightarrow{W_E}.\overrightarrow{curl}\,\vec{H}.d\Omega - \int_{(\Omega)} \overrightarrow{W_E}.Rm.\gamma_r.\vec{E}.d\Omega \qquad [10]$$

For the electromagnetic problem we choose the Galerkin's ponderation. We use the vector:

$$\left(\overrightarrow{\delta H}, \overrightarrow{\delta E}\right) \in (V)$$

The integral formulation becomes:

$$\int_{(\Omega)} \overrightarrow{\delta H}.\mu_r.\frac{\partial \vec{H}}{\partial t}.d\Omega = -\int_{(\Omega)} \overrightarrow{\delta H}.\overrightarrow{curl}\,\vec{E}.d\Omega \qquad [11]$$

$$\int_{(\Omega)} \overrightarrow{\delta E}.\varepsilon_r.\frac{\partial \vec{E}}{\partial t}.d\Omega = \int_{(\Omega)} \overrightarrow{\delta E}.\overrightarrow{curl}\,\vec{H}.d\Omega - \int_{(\Omega)} \overrightarrow{\delta E}.Rm.\gamma_r.\vec{E}.d\Omega \qquad [12]$$

The equations [11] and [12] constitute the *first formulation*. The integrals of the right hand side of [11] can be transformed by formula [13]:

$$\int_{(\Omega)} \overrightarrow{\delta H}.\overrightarrow{curl}\,\vec{E}.d\Omega = \int_{(\Omega)} \vec{E}.\overrightarrow{curl}\,\overrightarrow{\delta H}.d\Omega - \int_{(\Gamma)} \left(\overrightarrow{\delta H}\times\vec{E}\right)\vec{n}.d\Gamma \qquad [13]$$

We can use this capacity for the introduction of the *natural boundary conditions*. In that way we obtain the *second formulation* by transformation of the equation [11]:

$$\int_{(\Omega)} \overrightarrow{\delta H}.\mu_r.\frac{\partial \vec{H}}{\partial t}.d\Omega = -\int_{(\Omega)} \vec{E}.\overrightarrow{curl}\,\overrightarrow{\delta H}.d\Omega + \int_{(\Gamma)} \left(\overrightarrow{\delta H}\times\vec{E}\right)\vec{n}.d\Gamma \qquad [14]$$

$$\int_{(\Omega)} \overrightarrow{\delta E}.\varepsilon_r.\frac{\partial \vec{E}}{\partial t}.d\Omega = \int_{(\Omega)} \overrightarrow{\delta E}.\overrightarrow{curl}\,\vec{H}.d\Omega - \int_{(\Omega)} \overrightarrow{\delta E}.Rm.\gamma_r.\vec{E}.d\Omega \qquad [15]$$

3.2. *Finite Element formulation* [DHA 81]

Element i is called (Ω_i) and the principal properties are:

$$\bigcup(\Omega_i) = (\Omega) \quad \textit{and} \quad (\Omega_i)\bigcap(\Omega_j) = 0 \qquad i \neq j$$

In that way, we can formulate the geometrical discretization. For the analytical discretization we search an approximative solution in a subspace of (V) with finite dimensions (V_h). Let $n_i(x)$ a base of (V_h) and index n denotes the elementary nodal values. The approximate function can be written for an isoparametrical element [DHA 81]:

$$x_i^h = n_j.x_{ij}^n$$

$$H_i^h = n_j.H_{ij}^n \quad \text{and} \quad E_i^h = n_j.E_i^n$$

The discretization of the electric fields is as follows:

$$\{E_h\} = \begin{bmatrix} \langle n_i \rangle & \langle 0 \rangle & \langle 0 \rangle \\ \langle 0 \rangle & \langle n_i \rangle & \langle 0 \rangle \\ \langle 0 \rangle & \langle 0 \rangle & \langle n_i \rangle \end{bmatrix} \cdot \begin{Bmatrix} E_x^n \\ E_y^n \\ E_z^n \end{Bmatrix} = [N] \left\{ E^n \right\} \qquad [16]$$

So the discretization of the curl operator is easy and we have:

$$\overrightarrow{\text{curl}}\,\overrightarrow{E_h} = \begin{bmatrix} \langle 0 \rangle & -\left\langle \frac{\partial n_i}{\partial z} \right\rangle & \left\langle \frac{\partial n_i}{\partial y} \right\rangle \\ \left\langle \frac{\partial n_i}{\partial z} \right\rangle & \langle 0 \rangle & -\left\langle \frac{\partial n_i}{\partial x} \right\rangle \\ -\left\langle \frac{\partial n_i}{\partial y} \right\rangle & \left\langle \frac{\partial n_i}{\partial x} \right\rangle & \langle 0 \rangle \end{bmatrix} \begin{Bmatrix} E_x^n \\ E_y^n \\ E_z^n \end{Bmatrix} = [R] \left\{ E^n \right\} \qquad [17]$$

We have a similar relation for the magnetic field. This curl formulation denotes an anti-symmetrical operator [R].

In the Finite Element Method we try and secure an approximative solution of the weak formulation. We have the convergence in space (V):

$$\lim_{h \to 0} \| U - U_h \| = 0 \quad \text{with} \quad U = \left(\vec{E}, \vec{H} \right)$$

3.3. *Matricial formulation*

We define the following matrices:

$$[m] = \int_{(\Omega)} N^T.N.d\Omega \quad \text{the mass matrix}$$

$$[m_\mu] = \int_{(\Omega)} N^T.\mu_r.N.d\Omega \quad \text{the magnetic mass matrix}$$

$$[m_\varepsilon] = \int_{(\Omega)} N^T . \varepsilon_r . N . d\Omega \quad \text{the electric mass matrix}$$

$$[k_i] = \int_{(\Omega)} N^T . R . d\Omega \quad \text{the electric stiffness matrix}$$

The elementary electric loading $\{f_i\}$ where the electric field is known and is given by *natural boundary conditions*:

$$\{f_i\} = \int_{(\Gamma_0)} \begin{Bmatrix} \{n_i\}.E_0(y,t) \\ 0 \\ 0 \end{Bmatrix} . d\Gamma$$

All mass matrices are symmetrical.

For the full domain (Ω) the weak formulations [9] and [10] in the first case can be written :

$$\sum_{i=1}^{n} \left\langle \delta H^n , \delta E^n \right\rangle . \left(\begin{bmatrix} m_\mu & 0 \\ 0 & m_\varepsilon \end{bmatrix} . \begin{Bmatrix} \dfrac{\partial H^n}{\partial t} \\ \dfrac{\partial E^n}{\partial t} \end{Bmatrix} + \begin{bmatrix} 0 & k_i \\ -k_i & 0 \end{bmatrix} . \begin{Bmatrix} H^n \\ E^n \end{Bmatrix} \right) = 0 \qquad [18]$$

In that way we have a block-symmetrical electric stiffness matrix for the first formulation. For the second formulation, by discretization of equations [14] and [15] we obtain:

$$\sum_{i=1}^{n} \left\langle \delta H^n , \delta E^n \right\rangle . \left(\begin{bmatrix} m_\mu & 0 \\ 0 & m_\varepsilon \end{bmatrix} . \begin{Bmatrix} \dfrac{\partial H^n}{\partial t} \\ \dfrac{\partial E^n}{\partial t} \end{Bmatrix} - \begin{Bmatrix} f_i \\ 0 \end{Bmatrix} + \begin{bmatrix} 0 & -k_i^T \\ -k_i & 0 \end{bmatrix} . \begin{Bmatrix} H^n \\ E^n \end{Bmatrix} \right) = 0 \qquad [19]$$

In that way we build a symmetrical elementary electric stiffness matrix.

After a classical assembling operation where index (G) denotes the global values, the differential system is as follows:

$$[M].\frac{d}{dt}\begin{Bmatrix} H^{(G)} \\ E^{(G)} \end{Bmatrix} = \begin{Bmatrix} F_H^{(G)} \\ F_E^{(G)} \end{Bmatrix} - [K].\begin{Bmatrix} H^{(G)} \\ E^{(G)} \end{Bmatrix} \qquad [20]$$

where global matrix [M] is *symmetrical.* If the *second formulation* is used the global matrix [K] is also *symmetrical.* For the first formulation, the global electric loading is provided by the Dirichlet's conditions. Natural boundary conditions are also added for the second formulation.

3.4. *Numerical resolution*

The general formulation of the differential system is:

$$[M].\frac{d}{dt}\{U\} = \{F\} - [K].\{U\} \quad \text{where} \quad \{U\} = \left\{H^{(G)}, E^{(G)}\right\}$$

$$\frac{d}{dt}\{U\} = [M]^{-1}.\{\Psi(U,t)\} \quad \text{where} \quad \{\Psi(U,t)\} = \{F\} - [K].\{U\}$$

For the numerical time-resolution, several methods are tested [SOD 78].

For numerical quadrature points the nodes of the elements are chosen. Consequently, the mass matrix [M] is *diagonal.* This inversion is an easy procedure. It is a necessary condition for the efficiency of the methods above. Under these conditions we can test the explicit and implicit methods. In both cases we use a *matrix-free technique*, the mass matrix and the stiffness matrix never being built. We note a high performance level for the CPU and the storage costs.

3.4.1. *Semi-implicit method*

The corresponding algorithm is as follows:

$t_k = 0$

while ($t_k \le t_{max}$) :

$$\left\{ \begin{array}{c} \left\{\Delta U_k^i\right\} = \Delta t_k.\left[M_k^i\right]^{-1}.\left\{\Psi\left(U_k^i + \alpha.\Delta U_k^i, t_k + \alpha.\Delta t_k\right)\right\} \\ \left\{U_k^{i+1}\right\} = \left\{U_k^i\right\} + \left\{\Delta U_k^i\right\} \\ i = 1, 2, \ldots \quad \text{until} \left\|\Delta U_k^i - \Delta U_k^{i-1}\right\| \le \text{tolerence} \end{array} \right\}$$

$$t_{k+1} = t_k + \Delta t_k$$

end while

where α is the upward time-parameter.

The first method requires inner iterations for each time-step with index i for ΔU determination and the convergence criteria can be written [AND 84] :

$$\alpha . \Delta t . \left\| \frac{\partial}{\partial U} \left\{ [M]^{-1} . \Psi(U,t) \right\} \right\| < 1 \quad \text{let} \quad \Delta t < \Delta t_0$$

But we always find a time-step value for the convergence of the process. We note the good stability of the scheme in the implicit case. If α<0.5 a CFL condition is also required [DHA 81]. In this way we choose a time step as follows:

$$\Delta t \leq \text{Min}(\Delta t_0, \Delta t_{CFL})$$

In usual numerical tests these time step are similar.

We note specific cases :

– α=0 explicit method

– α=1 implicit method

– α=0.5 Crank-Nicholson scheme

The advantage of this method is the matrix free technique associated with an iterative method. The initial solution of each time step is close to the next solution. For the semi-implicit method the number of iterations is very low, two or three in practice.

3.4.2. *Runge-Kutta method*

The Runge-Kutta algorithm can be written:

$t_k = 0$

while $(t_k \leq t_{max})$:

$$t_k = t_k + \Delta t_k$$

end while

where λ_p and μ_p are the Runge-Kutta coefficients.

If the CFL condition is verified [AND 84], the Runge-Kutta method also gives satisfactory results. Both methods give similar numerical results. In practice, for the

numerical test, we use a semi implicit method and the Runge-Kutta method of 4th order. In the latter case, we have the following stability condition:

$$\Delta t \leq \frac{\Delta x_i}{c}$$

for the propagation phenomenon. The choice of the time-step presents several difficulties, because the CFL condition is complex especially if the spatial discretization is not uniform. Consequently a variable time-step is associated with the AMS technique described below.

3.5. *The code and the Automatic Multigrid System (AMS)*

We use efficient C++ Object Oriented Programming for the Finite Element code called FAFEMO (Fast Adaptive Finite Element Modular Object) developed by A. CHAMBAREL [CHA 97]. In this context, our numerical calculus uses a technique called the AMS. For all iterative or step-by-step processes, an expert system chooses the unknown degrees of freedom for the update of the solution, and the size of the unknown vector is optimized. The applications of this capability are very large:

- multiprocessor computing [CHA 97],
- wave front (in this paper),
- multidomain calculus (in this paper),
- moving boundary,
- multigrid simulation...

An expert system should be built for each problem. Mathematical, numerical and physical considerations can be used. Our example is easy and with the adimensional parameters we construct the expert system by the following method:

- first stage ($t<1$)

The wave front propagates with a celerity which is overvalued by 1. It stays in the wave guide and only the degrees of freedom between the electrodes are active:

- second stage ($t>1$)

The wave front propagates in the free space. The celerity of the electromagnetic wave preserves the same properties. The end of the line behaves like a source which emits in the free space.

full electric line active

$$d = \max\left(\sqrt{(y \pm a)^2 + (z-1)^2}\right)$$

$$\text{if } \left((d+1) \leq t\right) \Rightarrow \text{active degrees of freedom}$$

In our case the active degrees of freedom number increases with time.

The working of the AMS can be described by a matricial formulation. If the AMS expert system detects a constant domain (u_{ams}), the differential system becomes:

$$\begin{bmatrix} M_{ams} & 0 \\ 0 & M_{unk} \end{bmatrix} \cdot \frac{\partial}{\partial t} \begin{Bmatrix} U_{ams} \\ U_{unk} \end{Bmatrix} = \left\{ \begin{Bmatrix} f_{ams} \\ f_{unk} \end{Bmatrix} - \begin{bmatrix} K_{ams} & K_1 \\ K_2 & K_{unk} \end{bmatrix} \cdot \begin{Bmatrix} U_{ams} \\ U_{unk} \end{Bmatrix} \right\}$$

The 'ams' index concerns the choice of the expert system and the 'unk' index concerns the unknowns. After development, the differential system is as follows :

$$[M_{unk}] \cdot \frac{\partial}{\partial t} \{U_{unk}\} = \{f_{unk}\} - [K_2] \cdot \{U_{ams}\} - [K_{unk}] \cdot \{U_{unk}\}$$

$$\text{or } [M_{unk}] \cdot \frac{\partial}{\partial t} \{U_{unk}\} = \{f'_{unk}\} - [K_{unk}] \cdot \{U_{unk}\}$$

FAFEMO Object-Oriented Programming allows an easy building of the matricial system for each time-step. In that way we obtain a low size system.

These considerations are used for the implementation of the expert system. Initially the electromagnetic field is zero. Then the propagation starts. At that time, the AMS is active and the degrees of freedom in front of the wave front are disactivated. We obtain a range of time-dependent unknowns, and the process manages a low size problem. For time t_k, the time step Δt_k can be changed at each step with the CFL condition.

This constitutes a general Finite Element formulation for the Maxwell's equations with a symmetrical electric stiffness matrix.

4. Numerical results for 2D-TDR probe

4.1. *Space discretization*

The 2D model is presented in Figure 3. We discretize with triangular linear elements. They are described in literature references [DHA 81]. We refine the mesh near the electrodes (Figures 3, 4 and 5), so we have 13,985 triangular elements and 7,300 nodes. 29,200 differential equations are generated by the above Finite Element process. For time integration, we use a Runge-Kutta explicit method and a semi-implicit scheme for which the better upward parameter is α=0.75. This alpha value is a good compromise for the stability control of the scheme [SOD 78].

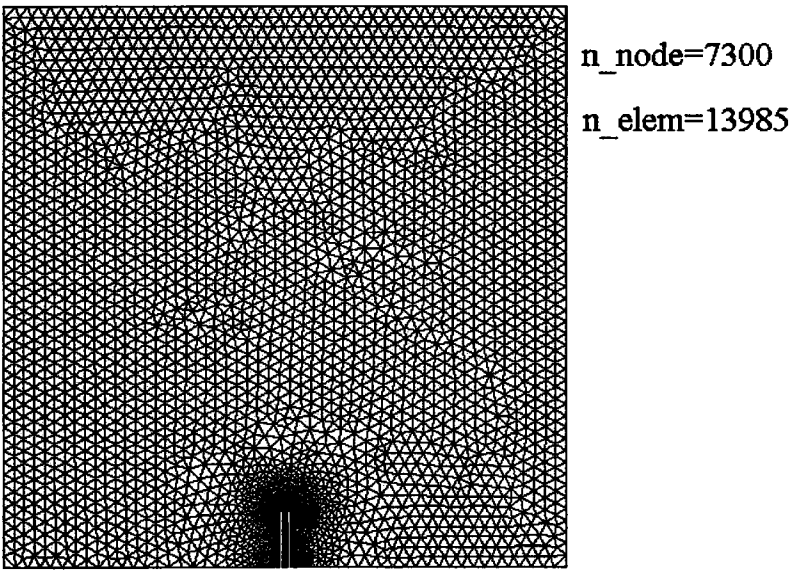

Figure 3. *Global mesh*

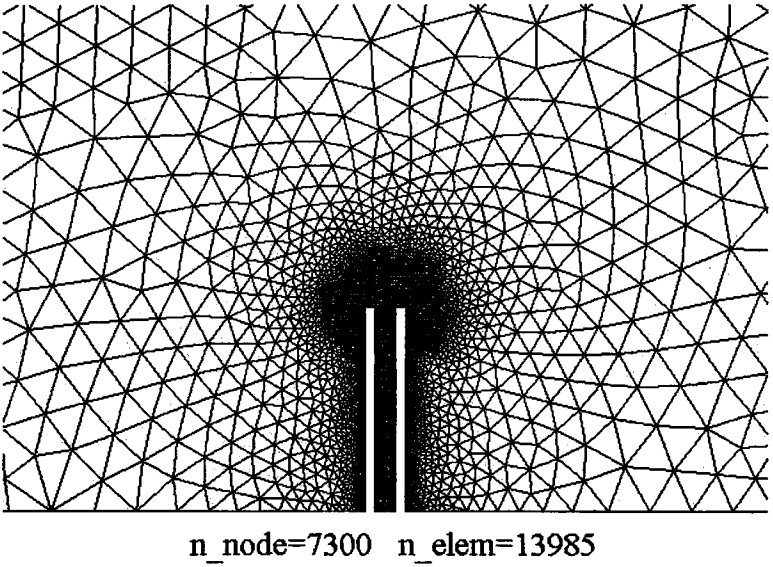

Figure 4. *Local mesh*

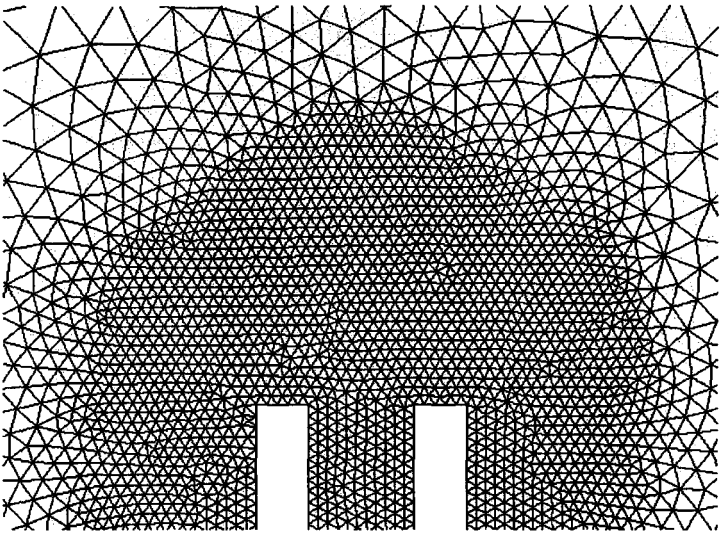

Figure 5. *Outlet zoom*

4.2. *Numerical results*

4.2.1. *Case of homogeneous space*

In this case, the electric properties are constant and isotropic (ε_0,μ_0). This case is considered as a benchmark for the calculus verification. In the following figures and for different times, the solution of the adimensional magnetic field or the adimensional electromagnetic energy are presented.

In Figures 6 and 7, the electromagnetic solution is presented at adimensional time t=0.5. We notice that the wave has reached the middle of the electric line. This is in accordance with the electromagnetic wave celerity. We also note a little spreading of the wave front because of the wave guide cut frequency, and also probably because of the numerical scheme.

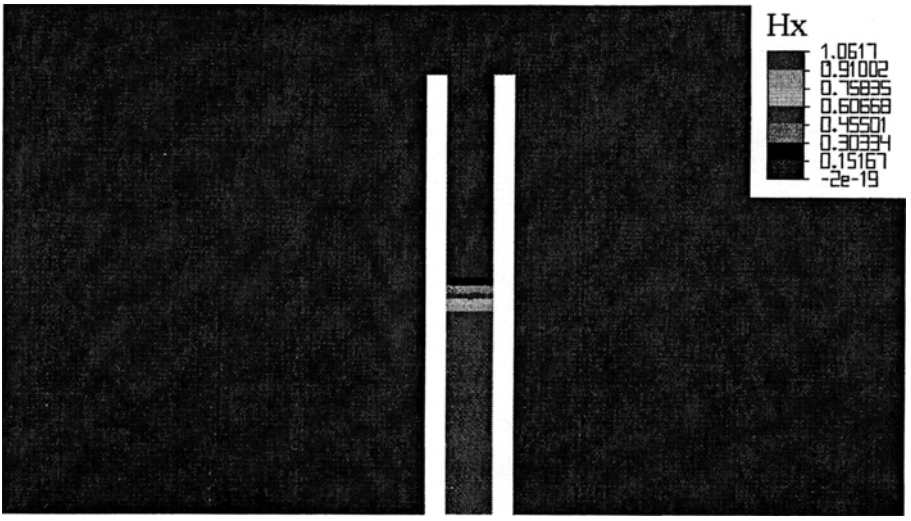

Figure 6. *Magnetic field iso-value*

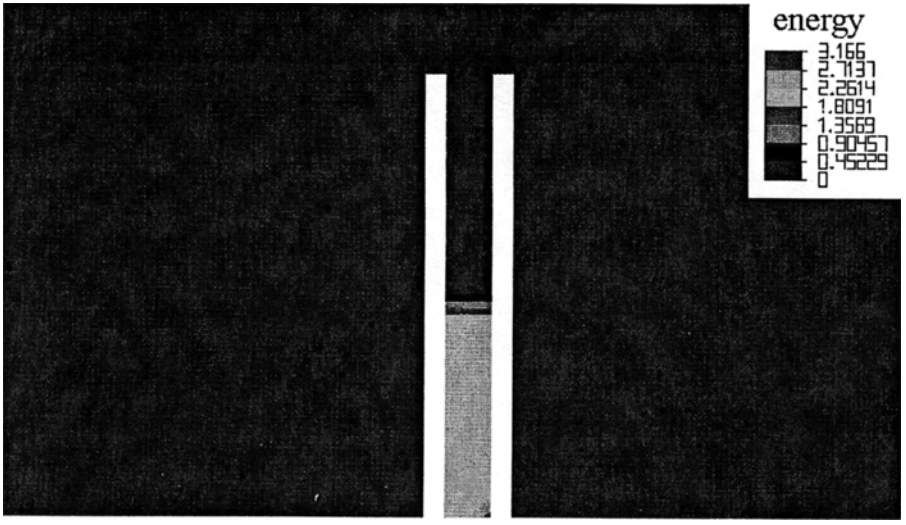

Figure 7. *Energy iso-value.*

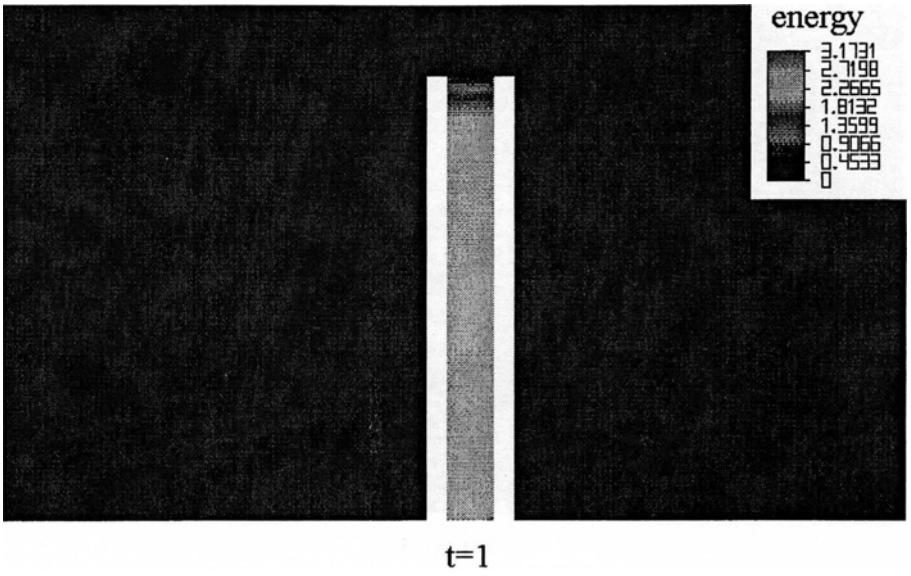

Figure 8. *Full wave guide*

Figure 8 shows the adimensional electromagnetic energy at time t=1. We notice that the electromagnetic field fills the full electric line. It is still in accordance with the electromagnetic wave celerity c.

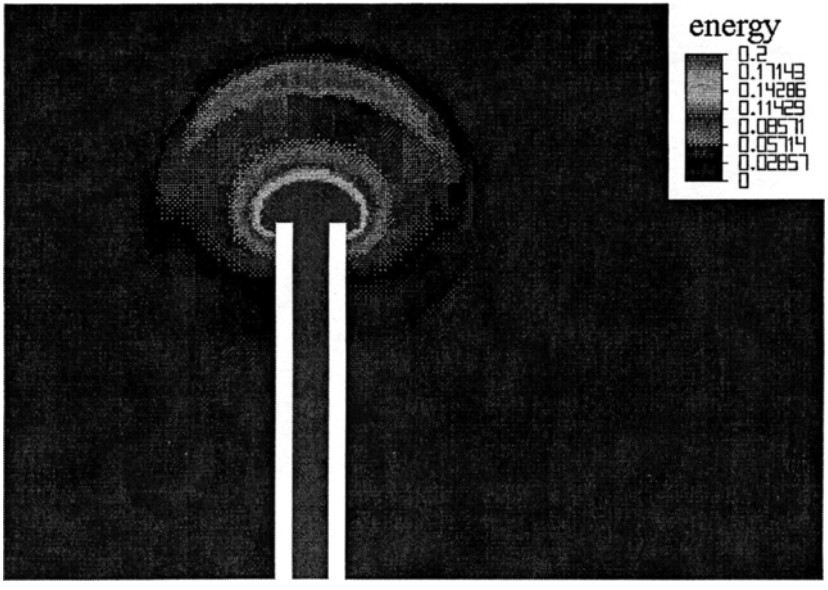

Figure 9. *Energy diffraction*

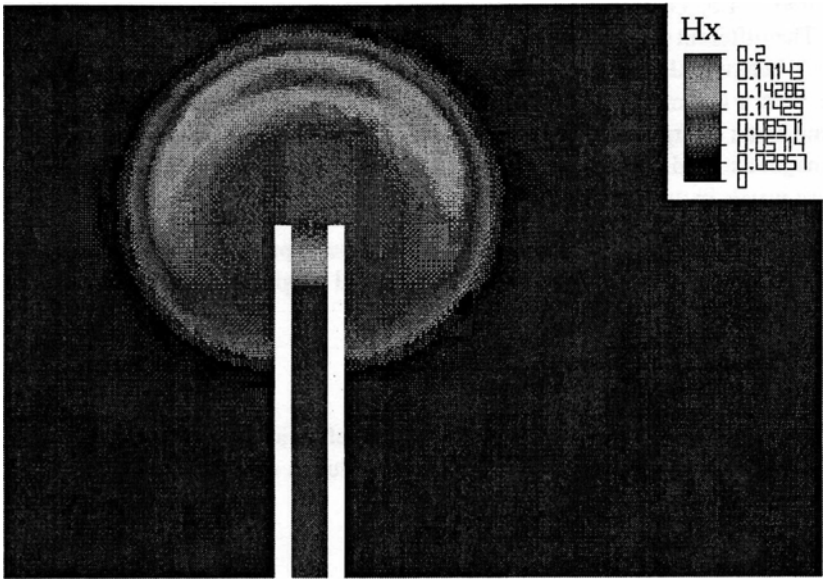

Figure 10. *Magnetic field*

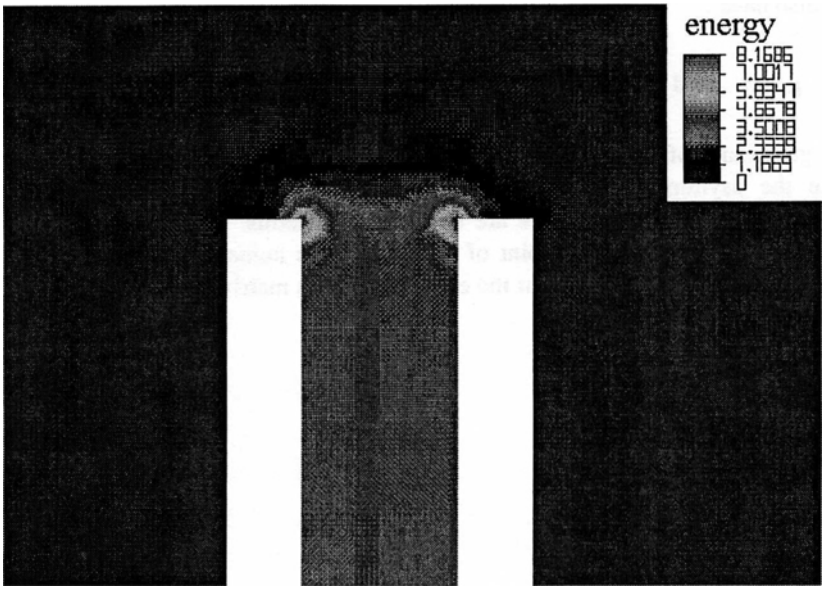

Figure 11. *Point effect*

At time t=1.5, coming of the electromagnetic wave in the external medium begins. The different results are presented in Figures 9 and 10. We note that the end of the line behaves like an electromagnetic source and the approximate wave front is a circle with a 0.5 radius. Figures 9 and 10 present only the low intensity of the electromagnetic energy and the magnetic field in order to highlight the external electromagnetic field. It focuses on the numerical values. In these conditions the stationary waves in the wave guide are here not visible.

The electromagnetic energy at the end of the line is presented in Figure 11. We note the well-known point effect at both internal angles because of the high intensity of the electric field.

4.2.2. *An example of variable electric properties*

In this case, we choose an example of variable electric properties. Around point (y_0, z_0) is a spot of electric singularity and the ε value is modified by the following mathematical model:

$$\varepsilon(y,z)=\varepsilon_0+\varepsilon_1 .\exp\left(-\frac{(y-y_0)^2+(z-z_0)^2}{a^2}\right)$$

We also have :

$$\mu_r=1 \quad \text{and} \quad Rm=0$$

The gaussian profile of ε is chosen. The example is presented in Figure 12 and we note the asymmetrical dielectric spot. Indeed, we are here considering a mathematical model in which there are no dissipative terms. We stand in the most unfavorable case from the viewpoint of stability of the numerical solution. In this case, there are no diagonal terms for the electric stiffness matrix.

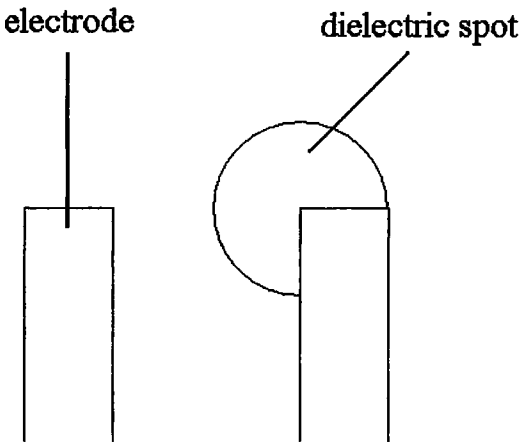

Figure 12. *Electric singularity*

Figures 13, 14 and 15 present the magnetic field at different times (1.5, 2.0, 3.0). If the time is greater than 1, then the electromagnetic field is at the end of the electric line. We notice stationary waves in the wave guide (Figure 15). This figure shows the coming out of the electromagnetic wave in the free space. We note a large dissymmetry because of the electric particularity of the medium. The celerity of the electromagnetic wave decreases strongly in that zone and a more important part of the wave is reflected toward the entrance of the wave guide. It therefore provokes a variation in the impedance of the electric line, in particular, as seen at the entrance.

Figure 16 show the AMS efficiency. The AMS disactivated boundary follows the wave front. In that way we have an increasing number unknowns.

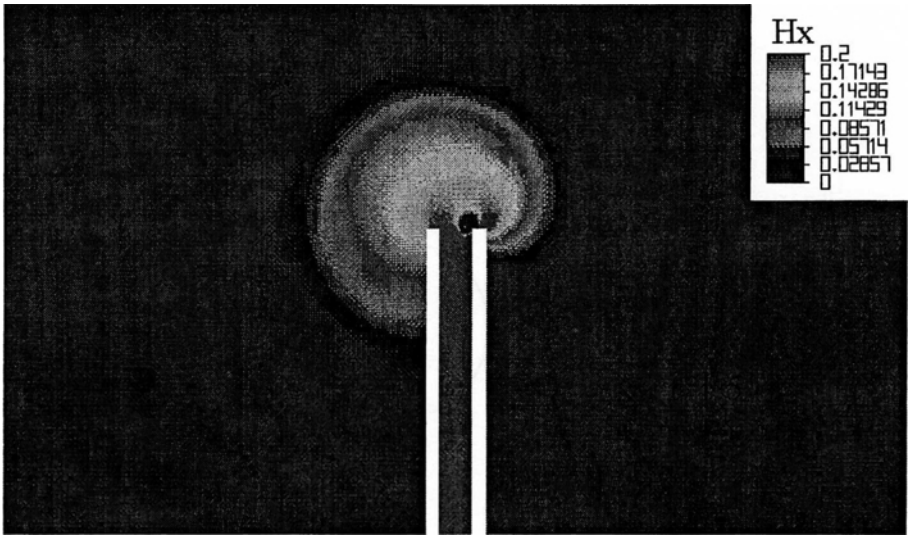

Figure 13. *Magnetic field asymmetry*

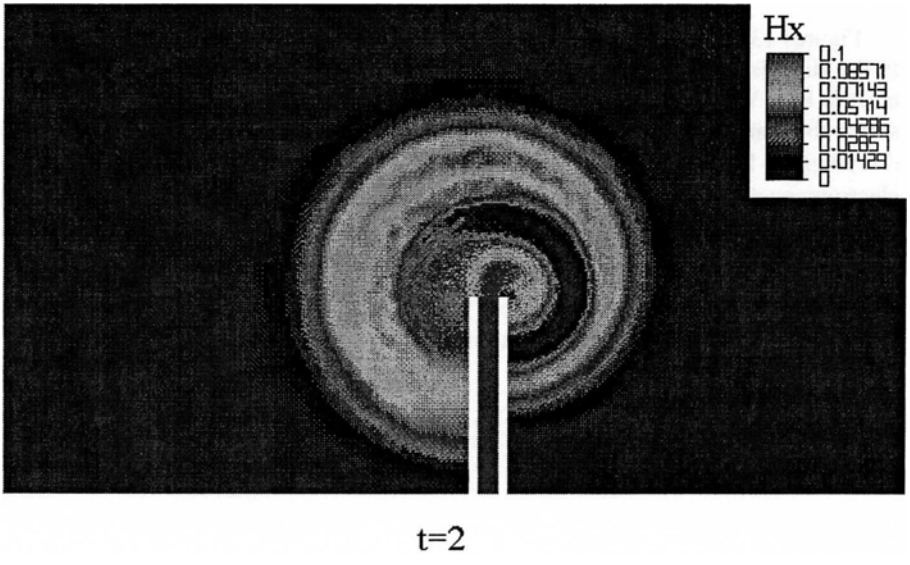

Figure 14. *Magnetic field asymmetry*

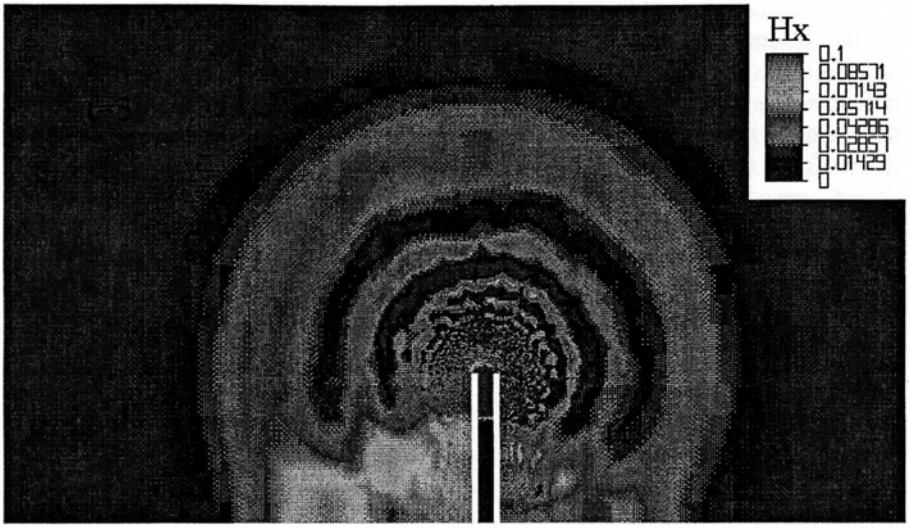

Figure 15. *Magnetic field asymmetry*

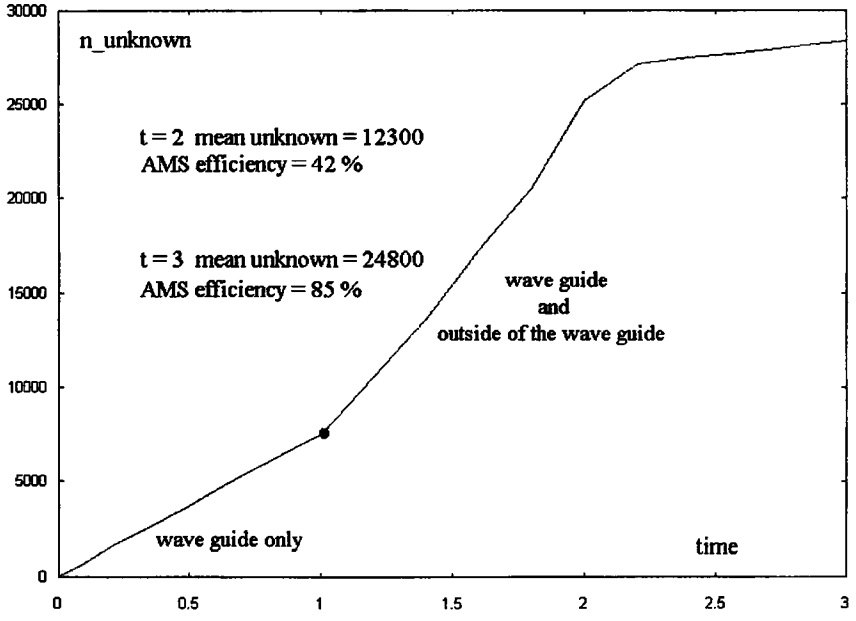

Figure 16. *AMS running*

The intensity at the top-end of the line is presented in Figure 17. The asymmetry of the electromagnetic field is also evident. We compare here the case of homogeneous electric properties with the existence of a dielectric spot. For the homogeneous medium with electric properties of the vacuum we note a spreading of the intensity signal because of the wave guide cut frequency. It is a low-frequency filter. If the time is lower than 1.5, we have a same line intensity after which the dotted curve shows the gap between the two cases. The two curves are first confounded until the wave, undergoing a reflection from the electric peculiarity comes back to the entrance. Measurement of this time gap allows the determination the distance of the dielectric singularity. Then, the analysis of the distorsion of the signal completes the knowledge of the peculiarity. At any rate through this analysis we have achieved a tool allowing the determination of a characteristic singularity catalog met in this type of problems.

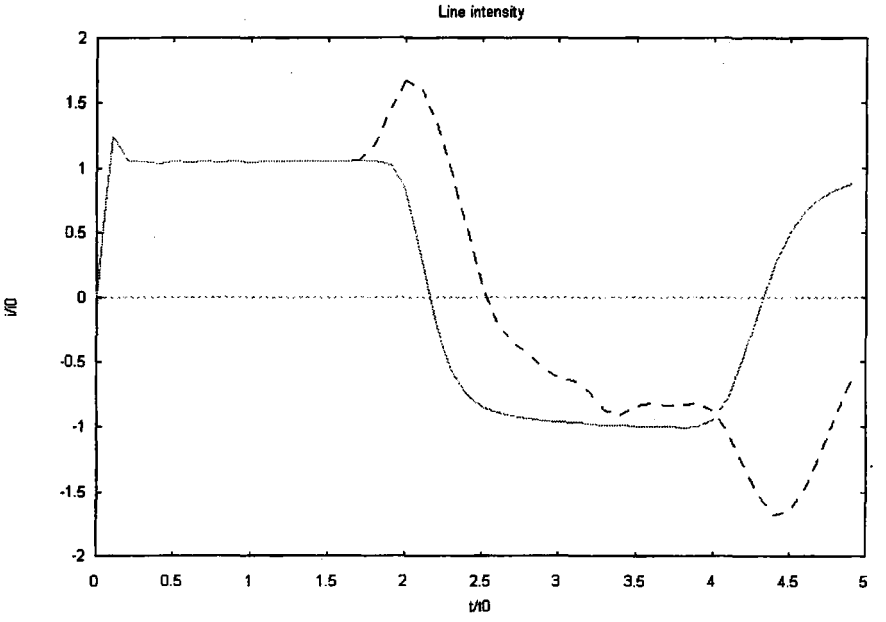

Figure 17. *Line intensity*

5. Conclusion

The TDR probe can be simulated by a Galerkin Finite Element approach. We present a general Finite Element formulation for Maxwell's equations in the case of propagation phenomenon and introduce the matricial structure of space discretization. We find and obtain a symmetrical matrix formulation. An electromagnetic wave propagates along the wave guide with the object determining

the variable electric properties of the space crossed. The electric loading is given by a natural boundary conditions. This process is performed by the AMS with a time dependent number of unknowns. The calculus are performed with a usual PC Pentium 200 MHz. In this way the CPU and memory cost are reasonable. Generally the wave propagation is always a difficult numerical problem. We do not detect instabilities [ASS 93] and this set of methods give good results. This paper show that the Finite Element Method is a good alternative to the FDTD (Finite Differences Time Domain) method that is currently used for this class of problems.

Acknowledgments

This work was supported by the French PNRH (Programme National de Recherche en Hydrologie), the INRA (Institut National de Recherche Agronomique) and the IUP/GMI (Institut Universitaire Professionalisé).

6. References

[AND 84] ANDERSON D.A., TANNEHILL J.C. and PLETCHER R.H., « Computational Fluid Mechanics and Heat Transfer », Hemisphere Publishing Corporation Editor, 1984.

[ASS 93] ASSOUS F., DEGOND P., HEINTZE E., RAVIARD P.A. and SEGRE J., « On a Finite Element Method for Solving the Three-Dimensional Maxwell Equations », *Journal of Computational Physics*, vol. 109, 1993, p. 222-237.

[CHA 97] CHAMBAREL A. and ONUPHRE E., « Parallel computation of an unsteady compressible flow », *Parallel Computing Technologies : Proceedings of the 4th International Conference*, Lecture Notes in Computer Sciences , vol. 1277, 1997, p. 377-382, V. Malyshkin edition, Springer.

[DAS 85] DASBERG S. and DALTON F.N., « Time domain reflectometry field measurement of soil water content and electrical conductivity », *Soil Scien. Am. Soc.*, vol. 49, 1985, p. 293-297.

[DHA 81] DHATT G. et TOUZOT G., *Une présentation de la méthode des éléments finis*, Editions Maloine S.A., 1981.

[DIR 93] DIRKSEN C. and DASBERG S., « Improved calibration of time domain reflectometry soil water content measurement », *Soil Scien. Am. Soc.*, vol.57, 1993, p. 660-667.

[DOS 97] DOS SANTOS L.A., « Développement d'une nouvelle méthode de détermination des profils de teneur en eau dans les sols par inversion d'un signal TDR », Thèse de doctorat, Université Joseph Fourier de Grenoble, 1997.

[FLE 85] FLETCHER ARMSTRONG C., LIGON J.T. and THOMSON S.J., « Calibration of Watermark model 200 soil moisture sensor », *Summer Meeting of American Society of Agricultural Engineers*, 1985, p. 1-11, Michigan State University.

[FLE 91] FLECKINGER E., *Electromagnétisme*, Editions Masson, Paris, 1991.

[GAU 93] GAUDU J.C., CHANZY A., MOHRATH D., « Mesure de l'humidité des sols par une méthode capacitive : analyse des facteurs influançant la mesure », *Agronomie*, vol. 13, n°1, 1993, p. 57-73.

[LUE 93] LUEBBERS R., *IEEE Transactions on Antennas and Propagation*, vol. 41, n° 11, 1993.

[SOD 78] SOD G.A., « A survey of Several Finite Difference Methods for Systems of Nonlinear Hyperbolic Conservation Laws », *Journal of Computational Physics*, vol. 27, 1978, p. 1-31.

[SPA 95] SPAANS E.J.A. and BAKER J., « Examining the use of Time Domain Reflectometry for measuring liquid water-content in frozen soil », *Water Ressources Research*, vol. 31, n°12, 1995, p. 2917-2925.

[TOD 98] TODOROFF P., « Modélisation de la propagation micro-ondes dans le sol afin d'obtenir un profil hydrique par réflectométrie temporelle », Thèse de doctorat, Université de la Réunion, 1998.

[VAN 63] VAN BAVEL C.H.M., « Neutron scattering measurement of soil moisture : development and current status », *Proc. Int. Symp. On humidity and moisture*, 1963, p. 171-184, Washington DC.

NOMENCLATURE

R	lineic resistance
L	lineic self induction
C	lineic capacitance
G	lineic conductance
V	scalar potential of electric field
I	electric intensity
Z_k	impedance
$\vec{E}$	electric field
$\vec{D}$	electric induction field
$\vec{B}$	magnetic induction field
$\vec{H}$	magnetic field
$\vec{S}$	Poynting vector
$\vec{A}$	vector potential of magnetic induction
$\vec{J}$	courant density
$\vec{n}$	normal vector
w	volumic energy
ρ	volumic density of electric charges

σ	surfacic density of electric charges
γ_r, γ_0	ohmic conductivity
Rm	magnetic Reynolds number
$\varepsilon_r, \varepsilon_0$	electric permitivity
μ_r, μ_0	magnetic permeability
c	light celerity
(Ω)	integration domain
x, y, z	cartesian coordinates
$\langle . \rangle$	line matrix
$\{.\}$	column matrix
Δt	time-step
(Ω_i)	element i
$\langle n \rangle$	lagrangian polynomial base
$[I]$	identity matrix
$[m_i]$	elementary mass matrix
$[M]$	global mass matrix
$[k_i]$	elementary stiffness matrix
$[K]$	stiffness matrix
$[f_i]$	elementary loading
$\{F\}$	global loading
α	upward parameter